electrochem

MDPI

Article

Coriaria nepalensis Stem Alkaloid as a Green Inhibitor for Mild Steel Corrosion in 1 M H_2SO_4 Solution

Hari Bhakta Oli [1], Jamuna Thapa Magar [1], Nawaraj Khadka [1], Anup Subedee [1], Deval Prasad Bhattarai [1,*] and Bishweshwar Pant [2,3,*]

[1] Department of Chemistry, Amrit Campus, Tribhuvan University, Kathmandu 44618, Nepal
[2] Carbon Composite Energy Nanomaterials Research Center, Woosuk University, Wanju 55338, Korea
[3] Woosuk Institute of Smart Convergence Life Care (WSCLC), Woosuk University, Wanju 55338, Korea
* Correspondence: deval.bhattarai@ac.tu.edu.np (D.P.B.); bisup@woosuk.ac.kr (B.P.)

Abstract: Using natural plant extracts on metallic substances is the most frequently studied green corrosion inhibition approach in corrosion science. In this work, *Coriaria nepalensis* Stem Alkaloid (CNSA) has been successfully extracted and characterized by qualitative chemical (Mayer's and Dragendroff's) test and spectroscopic (UV and FTIR) measurement. CNSA has been employed as a green inhibitor for Mild Steel (MS) corrosion subjected to 1 M H_2SO_4 solution. The corrosion inhibition efficacy has been assessed by weight loss and polarization measurement methods. The effect of inhibitor concentration, immersion period, and temperature on the inhibition efficiency for the MS immersed in both acid and inhibitor solutions of different concentrations have been investigated. The maximum inhibition effect observed for CNSA is 96.4% for MS immersed in 1000 ppm inhibitor solution for 6 h at 18 °C by the weight loss measurement method. Similarly, the polarization measurement method observed a 97.03% inhibition efficiency for MS immersed for 3 h. The adsorption of inhibitor molecules on the MS surface aligns with the Langmuir model. The free energy of adsorption obtained is −28.75 kJ/mol indicating physical adsorption dominance over chemical adsorption. These findings suggested that CNSA has greater potential as an efficient green inhibitor.

Keywords: *Coriaria nepalensis*; alkaloid; green inhibitor; mild steel; weight loss; polarization

Citation: Oli, H.B.; Thapa Magar, J.; Khadka, N.; Subedee, A.; Bhattarai, D.P.; Pant, B. *Coriaria nepalensis* Stem Alkaloid as a Green Inhibitor for Mild Steel Corrosion in 1 M H_2SO_4 Solution. *Electrochem* **2022**, *3*, 713–727. https://doi.org/10.3390/electrochem3040047

Academic Editor: Masato Sone

Received: 21 September 2022
Accepted: 17 October 2022
Published: 1 November 2022

1. Introduction

Corrosion is a natural phenomenon and can be regarded as the degradation or deterioration of a substance, usually a metal, and its properties, over a period due to environmental exposure [1]. Mild steel (MS) is one of the iron alloys with several mechanical properties, making it a suitable material for industrial and machinery purposes. It is readily available, inexpensive, and very simple to fabricate and weld [2]. It has numerous applications in structural steel, automobiles, furniture and decorations, wire and fencing, nails, etc. The primary issue most commonly encountered while using MS is their susceptibility to corrosion, regardless of the nature of the environment [3]. Therefore, various materials and methods have been devised to cope with corrosion to minimize its effects [4].

Nevertheless, such methods are limited to processes like acid pickling, cleaning boilers, and descaling, where an acid solution is extensively used [5,6]. The residual acid in these processes may cause extensive corrosion damage. Such corrosion processes can be minimized using varieties of chemical inhibitors. Inhibitors used in the processes may be synthetic or natural. However, most synthetic organic compounds as inhibitors have been proven to be toxic to the environment, ecology and expensive chemicals [7,8]. However, green inhibitors could be the best alternatives regarding availability, sustainability, toxicity, cost-effectiveness, and environment [9]. Some green inhibitors have even exhibited comparable inhibitory effectiveness to conventional organic and anodic inhibitors [10]. Green inhibitors are the natural products of plant extract obtained from all the plant parts,

i.e., leaves, bark, fruits, flower, seeds, and roots. Plant extracts are rich in phytochemical constituents, among which heteroatoms (P, S, N and O) containing phytochemicals are the potential candidate for green inhibitors. These compounds are large organic molecules containing hetero atoms as active centers in conjugation with multiple bonds or aromatic rings [11]. Moreover, most natural products containing functional groups of the sort NH_2, C=O, and CHO are known to be viable inhibitors [12]. These compounds get adsorbed on the metal surface through the thermodynamically spontaneous adsorption processes to form a protective/defensive thin layer.

Various studies on green corrosion inhibitors based on crude (methanol extract) have been reported. However, very few reports on corrosion inhibition using alkaloid extract can be found elsewhere. Some recent studies are listed in Table 1.

Table 1. Plants and their alkaloids as green corrosion inhibitors.

S.N.	Plant Name	Metal	Medium	Method	I.E. (%)	Conc.	Reference
1.	*Caulerpa racemose*	MS	1 M HCl	Weight loss Polarization EIS	83 80 85	100 ppm 25 ppm 25 ppm	[13]
2.	*Ochrosia oppositifolia*/Bark & leaves	MS	1 M HCl	Polarization EIS	94 89–90	20–25 ppm 25 ppm	[14]
3.	*Neolamarckia cadamba*/Bark & leaves	MS	1 M HCl	Polarization EIS	89 83	5 ppm	[15]
4.	*Garcinia kola*/Seed	MS	5 M H_2SO_4	Weight loss Hydrogen evolution	98.8 99.4	10 g/L	[16]
5.	*Solanum melongena*/Leaves	Carbon steel	Na_2CO_3	Weight loss	81.1	3 g/L	[17]
6.	*Geisso spermum* leave	C38 steel	1 M HCl	Polarization	92	100 ppm	[18]
7.	*Rauvolfia macrophylla*/Bark	C38 steel	1 M HCl & 0.5 M H_2SO_4	EIS Polarization	97, 93 92, 93	200 ppm	[19]
8.	*Retama monosperma*/Seed	Carbon steel	1 M HCl	Electrochemical	94.42	400 ppm	[20]
9.	*Rychnostilus retusa*/Rhizome	MS	1 M H_2SO_4	Weight loss Polarization	87.51 93.24	1000 ppm	[5]
10.	*Artemisia vulragis*/Stem *Solanum tubersum*/Stem	MS MS	1 M H_2SO_4 1 M H_2SO_4	Weight loss Polarization Weight loss Polarization	92.58 88.06 90.79 83.22	1000 ppm	[21]
11.	*Alnus nepalensis*/Bark	MS	1 M H_2SO_4	Weight loss Polarization	71.94 78.48	1000 ppm	[6]
12.	*Annona Squamosa*/Leaves & seed	C38	1 M HCl	Polarization EIS	84 92	100 ppm	[22]
13.	*Palicourea guianensis*/Leaves	C38	1 M HCl	Polarization EIS	88 89	100 ppm	[23]
14.	*Guatteria ouregou*/leaves *Simira tinctoria*/Bark	C38 C38	0.1 M HCl 0.1 M HCl	Polarization EIS Polarization EIS	88 92 90 92	250 ppm	[24]
15.	*Acacia catechu*/Bark	Mild Steel	1 M H_2SO_4	Weight loss Polarization	93.96 98.54	1000 ppm	[25]
16.	*Taxus buccata*/Areal	Carbon Steel	1 M HCl	Weight loss Polarization EIS	83.85 84.49 86.12	200 ppm	[26]
17.	*Alstonica angustifolia var. latfolia*/leaves	Mild Steel	1 M HCl	Polarization EIS	84 88	5 mg/L	[27]

Coriaria nepalensis is a common native shrub of the Coriariaceae family that grows around 1.5–2.5 m tall and is found in the western part of Nepal. The plant possesses rapid

growth and higher environmental adaptability. The vegetative parts of the plant and fruit twig are shown in Figure 1.

(**a**) (**b**)

Figure 1. (**a**) Vegetative part of the plant and (**b**) fruit twig.

The sodium hydroxide extract of *Coriaria nepalensis* bark showed a significant amount of tannin and is reported to be a renewable source [28]. The methanolic extract has been reported to be more bacteriostatic than essential oil obtained from the leaves of this shrub [29]. The chloroform extract obtained from this plant's root is exploited to isolate new compounds such as sesquiterpene lactone, corialactone E, neolignan, coriarianeolignan, and apocarotenoids [30]. Among many phytochemicals, 4-Pyrimidinecarboxylic acid and Dihydrocorynantheine are the two most common alkaloids in *C. nepalensis* given in Scheme 1 [29,31].

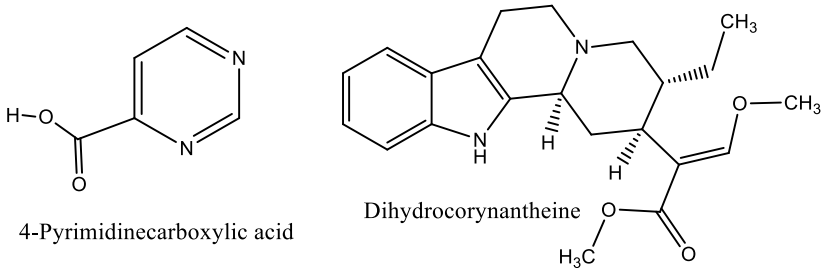

Scheme 1. Alkaloids of *Coriaria nepalensis*.

2. Materials and Methods

2.1. Chemicals and Instruments Used

The chemicals used in this experiment were all laboratory grade, and no additional purification was done. Sulfuric acid (Fischer Scientific, Maharastra, India, 97%, sp. gr. 1.835), oxalic acid (Fischer Scientific, Maharastra, India, 99%), and NaOH (Merck life Science, Karnatak India 97%) were used to prepare corrosive media. Dichloromethane (Galaxo Laboratories, Mumbai, India, sp. gr. 1.326), methanol (Thermo Fischer Scientific, Maharastra, India, sp. gr. 0.792), tartaric acid (RANBAXY Lab., Haryana India, 99.0%), and ammonia (Sisco Research Lab., Mumbai, India, sp. gr. 0.91) were used to extract alkaloids. The instruments used were UV (Labotronics, Haryana, India, LT-2808), FTIR (Perkin Elmer Waltham, USA 10.6.2), a rotary evaporator (IKA 10), a Digital Vernier Caliper and a Hokuto Denko Potentiostat (HA-151) were used as analytical tools.

2.2. Extraction of Alkaloids from Coriaria nepalensis Stem

The stem of *Coriaria nepalensis* (Machhaino) was collected from Bagarkot, (Latitude: 29.24″ and Longitude: 80.45″; 29°17′54.4″ N 80°27′59.2″ E), Dadeldhura, Far-western

Province, Nepal. The plant's shade-dried and finely ground stem was soaked in hexane for 24 h to eliminate the unsaturated organic compounds followed by fat dissolution and filtration. The as-obtained residue was macerated in 700 mL of methanol for seven days and filtered. A methanol extract as a filtrate was obtained and acidified using 5% tartaric acid (pH < 3.5) to protonate the 1°, 2°, and 3° alkaloids and filtered. After that, the ammonia solution was added (pH > 10) for the deprotonation to obtain deprotonated alkaloids with lone pair electrons. Then, a separating funnel separated the alkaloids from this alkaline solution using dichloromethane (DCM). The lower green slurry of the DCM layer of alkaloids was obtained and concentrated using a digital rotatory evaporator, followed by drying in a water bath (<40 °C). A dry alkaloid of *Coriaria nepalensis* was obtained.

The dry alkaloids were characterized by Mayer's and Dragendroff's tests followed by a FTIR spectroscopic test method.

2.3. Preparation of MS Specimen

The MS coupons of equal dimensions and varying weight were collected from the local market. To obtain a clean and reproducible surface, each coupon was polished with silicon carbide paper of different grit sizes (i.e., 100, 200, 400, 600, 800, 1000, and 1200) and then washed with hexane. Then, the coupons were sonicated in ethanol for 30 min, dried, and their dimensions were measured with the help of a digital Vernier Caliper before each weight loss experiment.

2.4. Preparation of Inhibitor Solution

To prepare the stock solution of inhibitor 1 g of alkaloid was dissolved in 100 mL of 1M H_2SO_4 and filtered to remove the un-dissolved particles. Then, the filtrate was taken in a 1000 mL volumetric flask and diluted up to the mark by 1 M H_2SO_4, which was taken as a 1000 ppm of stock solution from which different concentrations (200, 400, 600, and 800 ppm) of inhibitor solutions were prepared by the serial dilution method.

2.5. Weight Loss Measurement Method

It is a simple quantitative method of dealing with the relationship between time and weight by recording the difference in weight over specific time intervals. To study the effect of immersion time, the effect of inhibitor's concentration and adsorption isotherm MS specimens were exposed to a corrosive and inhibitor media for a certain time, and subsequent measurements were carried out. Mathematically, the inhibition efficiency and fraction of the surface covered by alkaloids were estimated as per Equations (1) and (2) [21].

$$\text{Inhibition Efficiency (IE) \%} = \frac{W_0 - W_i}{W_0} \times 100 \quad (1)$$

$$\text{Fraction of surface coverage } (\theta) = \frac{W_0 - W_i}{W_0} \quad (2)$$

where W_0 = weight loss of mild steel in the absence of an inhibitor; W_i = weight loss of the mild steel in the presence of an inhibitor.

2.6. Electrochemical Measurement

The electrochemical measurements were carried out using a three-electrode cell setup connected to a Hokuto Denko Potentiostat (HA-151). The working electrode was an MS coupon, the counter electrode was graphite, and the reference electrode was a saturated calomel electrode (SCE). Before measuring the polarization of the sample, an equilibrium potential was achieved by conducting the OCP measurement for 30 min, followed by the cathodic and anodic polarization in the potential range of 0.8 to –0.2 (V). The polarization measurements were performed on MS samples in various inhibitor concentrations and in acid solution under 3 h in immersed circumstances. Tafel slope, corrosion potential,

and corrosion current were computed using the polarization curves. Using the formula in Equation (3), the corrosion inhibition efficiency was computed [21]:

$$\text{Inhibition efficiency (IE\%)} = \frac{I_{corr} - I*_{corr}}{I_{corr}} \times 100 \quad (3)$$

where Icorr and I*corr are the corrosion current density in the absence and presence of an inhibitor.

3. Results

The corrosion-inhibitory behavior of the alkaloids was studied using weight-loss and electrochemical methods. Initially, the CNSA was characterized by a qualitative chemical test and UV and FTIR spectroscopic measurements.

3.1. CNSA Characterization

3.1.1. Test of Alkaloids

Different qualitative tests for the confirmation of CNSA were performed. Different tests, as tabulated in Table 2, confirmed the presence of alkaloids.

Table 2. Confirmatory test for *Coriaria nepalensis* stem alkaloids.

S.N.	Experiment	Observations	Result
1.	Mayer's Test	The appearance of the orange precipitate.	Positive
2.	Dragendroff 's Test	The appearance of orange-red color.	Positive

There were large numbers of alkaloid molecules in the mixture. These alkaloids can form a complex with the reagents, thus forming a colored precipitate. For simplicity, the reactions involved in the phytochemical screening of alkaloids are represented in the reference of 4-Pyrimidinecarboxylic acid as in Scheme 2 [5,29]:

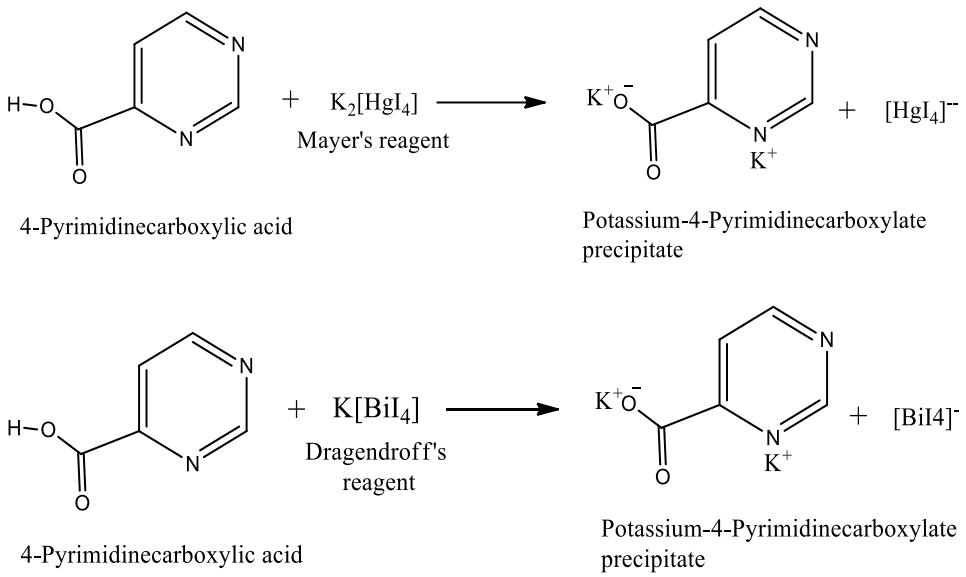

Scheme 2. Possible chemical reactions in the alkaloid test.

3.1.2. FTIR Spectroscopic Measurement

The type of bonding, π-bond conjugate system, functional group, and aromatic and aliphatic structures present in the organic compounds are identified by FTIR measurement. In the FTIR spectrum of CNSA (Figure 2), a broad band at 3250–3500 cm^{-1} appeared due to the overlapping combination of O-H and the amine group. A peak at 1706 cm^{-1} between

1540–1870 cm^{-1} was observed, indicating the carbonyl group's presence. The peaks at 2914 cm^{-1} and 2854 cm^{-1} were due to the C-H aliphatic asymmetry stretching vibration along with the methyl and methylene groups. The N-H bending vibration of the primary amine created peaks at 1612cm^{-1} and 1517cm^{-1}. A peak at approximately 1170 cm^{-1} and a broad peak at approximately 1072 cm^{-1} were due to C-N stretching of amines, and a peak at approximately 623 cm^{-1} was due to N-H bending vibration of primary and secondary amine [5,21,32].

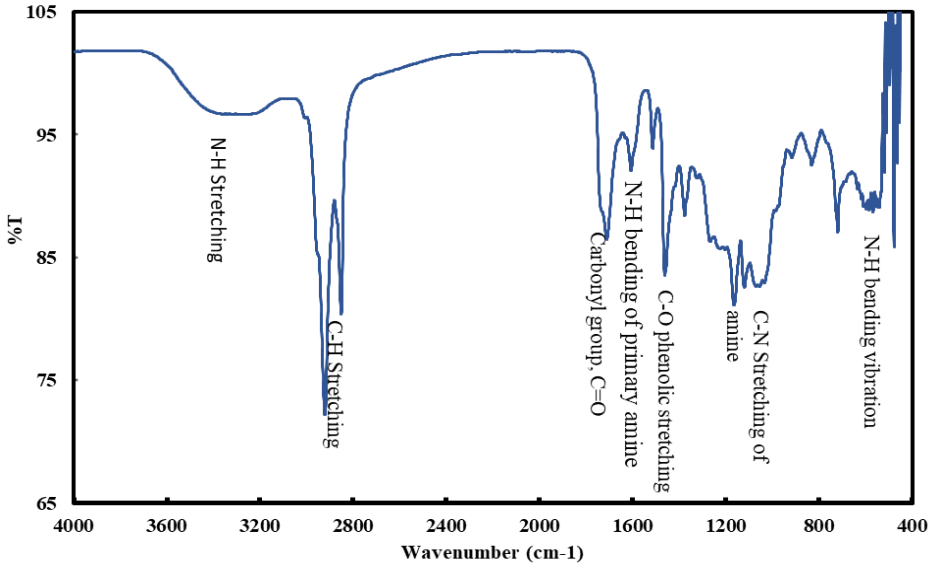

Figure 2. FTIR spectrum of CNSA.

3.1.3. UV Spectroscopic Measurement

The UV measurement identifies the unsaturation or presence of lone pair of electrons in the organic compounds. The sharp peak at 340 nm is due to the n–π* transition, whereas the sharp peak at 422 is due to the alkaloids' π–π* transition (Figure 3). If 4-Pyrimidinecarboxylic is taken as a reference, then these two sharp peaks indicate the presence of an aromatic ring containing N as a hetero element and the polyphenolic group in the structure [25,32,33].

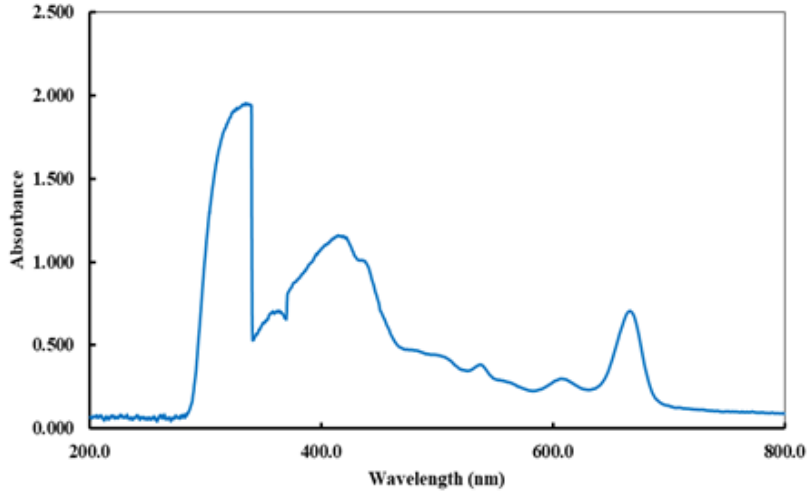

Figure 3. UV-Visible spectrum of CNSA.

3.2. Weight Loss Measurement

3.2.1. Effect of Immersion Time

The results showed that the weight loss (expressed in gram per unit area) of MS dipped in the solutions of 1 M H_2SO_4 in the presence of the inhibitor was lower compared to that dipped in 1 M H_2SO_4 solution for different time intervals (i.e., 0.5, 1, 3, 6, and 24 h). From Figure 4a, it was observed that the weight loss of MS for half an hour of immersion time is very small in all different inhibitor concentrations. However, the corresponding inhibition efficiency was not so high, possibly due to incomplete surface coverage of MS by inhibitor molecules. In all cases, the weight loss increases with increasing immersion time, while the inhibitor's effectiveness increases and then begins to decline after six hours. This is probably due to the subsequent desorption process. During adsorption, an inhibitor is assumed to produce a thin protective layer or barrier against corrosive molecules, while a desorption process is manifested due to the large size and orientation of the inhibitor molecule. Here, with an increase in time, the availability of the inhibitor molecules decreased due to the formation of a metal inhibitor chelate complex, which consequently led to a decrease in IE [6,21].

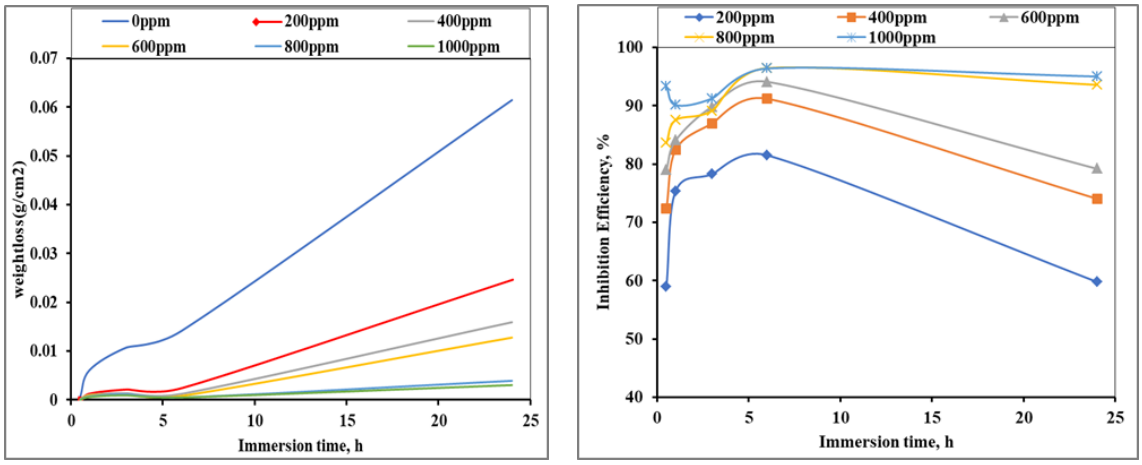

(**a**) (**b**)

Figure 4. Effect of immersion time on the variation of (**a**) weight loss and (**b**) inhibition efficiency for the corrosion of MS dipped into acid and different concentrations of inhibitor solution at room temperature.

From Figure 4b, it was found that the inhibition efficiency of the 1000 ppm CNSA is the highest (i.e., 96.41% for 6 h immersion time), which resulted in the lowest weight loss in the MS sample. At 24 h of immersion time, MS showed the highest weight loss in both acid and inhibitor media due to both desorption and structural defects on the inhibitor layer that allowed the interaction between the aggressive environments with the active MS surface. However, in a concentrated inhibitor solution, viz. 1000 ppm and 800 ppm solution, IE remains almost the same due to the availability of inhibitor molecules even up to a long time.

3.2.2. Effect of CNSA Concentration

The MS surface nature, operating temperature, and concentration of inhibitor molecules in the solution significantly influence the corrosion kinetics and its products, which subsequently affects the weight loss of MS samples. From Figure 5a, it was observed that the weight loss (g/cm^2) of MS decreased with an increase in the inhibitor's concentration. The result showed a minimum and maximum weight loss for MS in a 1000 ppm CNSA and acid solution.

From Figure 5b, the 200 ppm CNSA showed almost negligible inhibition efficiency for all immersion times, indicating the insufficiency of inhibitor molecules to cover the MS surface. However, the inhibition followed an increasing order with the increase in inhibitor

concentration. In this experiment, the optimum concentration for the highest inhibition was 1000 ppm CNSA solution, which showed more than 90% of inhibition up to 24 h.

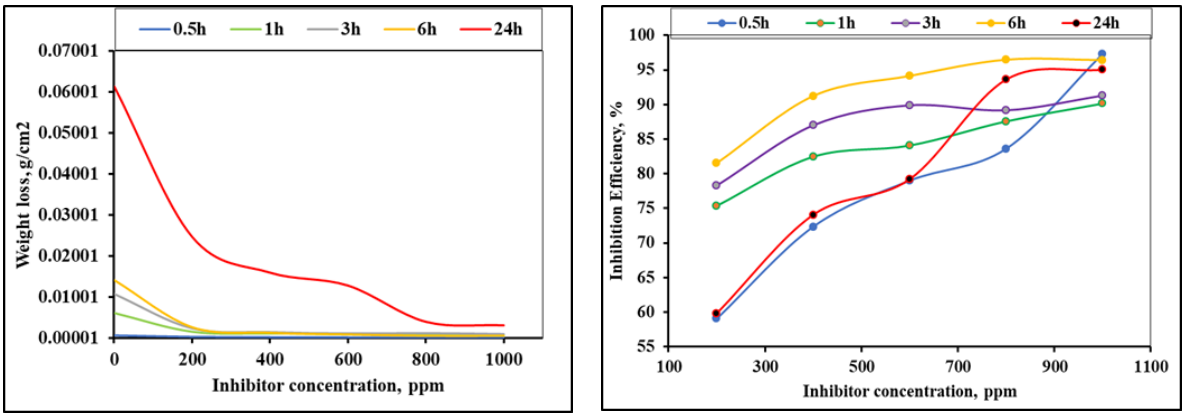

(**a**) (**b**)

Figure 5. Effects of different concentrations of CNSA on (**a**) weight loss and (**b**) inhibition efficiency for the mild steel corrosion in 1 M H_2SO_4 solution at various immersion times.

3.2.3. Adsorption Isotherm

For the basic concept of the interaction between the inhibitor and MS surface, Langmuir adsorption isotherms were examined. The adsorption of inhibitor molecules from an aqueous solution follows a quasi-substitution process, i.e., the replacement of initially adsorbed water molecules by inhibitor molecules. For reference, the 4-Pyrimidinecarboxylic acid molecule was taken to calculate the molar concentration of the inhibitor solution. However, it may not be the significant alkaloid responsible for the inhibition. The manifestation of adsorption, i.e., monolayer or multilayer, is determined by Langmuir's adsorption isotherm equation [34–36]. The linear relation between the fraction of covered surface (θ) and molar concentration (C) should be known to find the adsorption isotherm. If the slope of the curve is obtained by plotting $\frac{c}{\theta}$ vs. C in Equation (4) is unity, then it indicates the monolayer adsorption:

$$\frac{c}{\theta} = \frac{1}{k} + c \tag{4}$$

A plot of $\frac{c}{\theta}$ vs. C from Equation (4) gives a straight line with a R^2 value equal to 0.9998 and slope of 0.9872 as shown in Figure 6. This value is close to unity, indicating that inhibitor molecules' adsorption on the MS surface obeys the Langmuir adsorption isotherm [34,35]. Therefore, the adsorption may have occurred through mono- and multilayer formation. However, a complete monolayer produces before the multilayer formation. From the intercept of a graph, the value of K was calculated and found to be 2500. To determine the Gibb's free energy, the following equation was used:

$$G = -RT\ \ln(55.5 \times K) \tag{5}$$

where K = constant whose value is taken from Langmuir equations. It is equal to 2500 in this experiment. The working temperature is 19 °C, i.e., 292 K, and R = 8.314 J K^{-1} mol^{-1}. Substituting all the values in Equation (5) and calculating the free energy value obtained is equal to −28.75 kJ/Mol.

The negative value of free energy indicates that the process is spontaneous. The value of free energy of the adsorption is intermediate, i.e., in between the physical adsorption (i.e., >20 kJ/mol) and chemical adsorption (i.e., <40 kJ/mol). This implies that the adsorption process is physically dominant chemical adsorption.

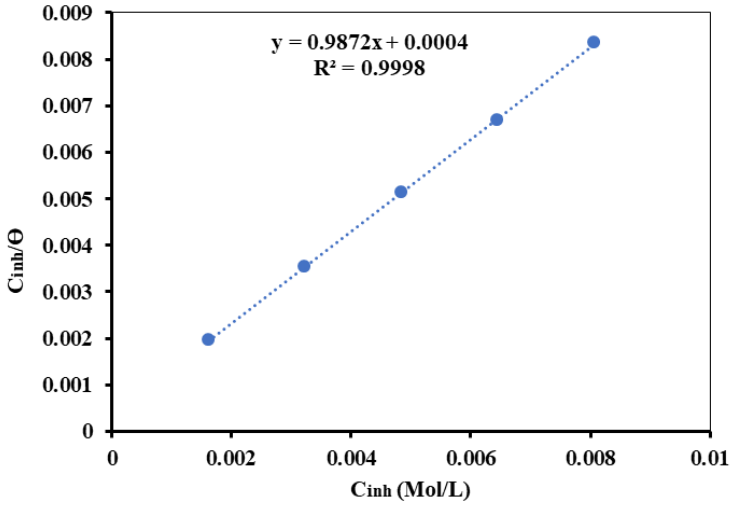

Figure 6. Langmuir adsorption isotherm plot for MS in 1 M H_2SO_4 with different inhibitor concentrations.

3.3. Electrochemical Measurement

Polarization Curves

The polarization of MS samples in both acid and inhibitor media was accomplished by applying ±350 mV in both anodic and cathodic directions using a potentiostat. This polarization measurement of the as-immersed MS was carried out at 18 °C laboratory temperature. From the Evans diagram and Tafel extrapolation (Figure 7), the current density of MS became diminished with the addition of an inhibitor. This is due to the surface coverage of MS by inhibitor molecules causing a reduction in the active sites for the attack by corrosive media.

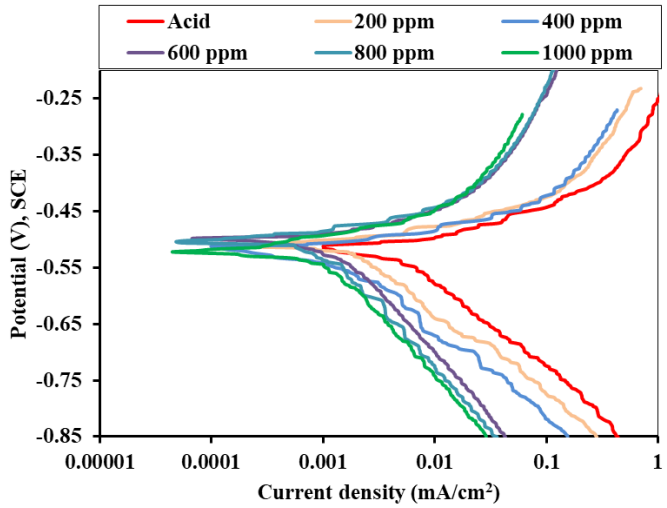

Figure 7. Potentiodynamic polarization curves for mild steel in 1 M H_2SO_4 containing different concentrations of the inhibitor as-immersed condition.

The electrochemical parameters, such as OCP, anodic and cathodic slope, corrosion current, and inhibition efficiency from the polarization curve, are recorded in Table 3.

Similar measurements were carried out after immersion of the MS coupons in different solutions at 3 h, as shown in Figure 8. The current density was found to be decreased from a corrosive media to increasing inhibitor concentrations which may be due to increased corrosive resistance of MS in inhibitor media. Similar to the as-immersed condition, the lowering of current density is due to similar reasons. This consequence of the reaction in the small surface area of MS produces a small current density. This implies that the alkaloid used in this experiment functioned as a good inhibitor.

Table 3. Anodic and cathodic slope and inhibition efficiency for as-immersed sample.

Medium	OCP (V)	Anodic Slope (V/decade)	Cathodic Slope (V/decade)	I_{corr} (mA/cm^2)	I. E. (%)
Acid	−0.529	0.00533	−0.147	0.0205	-
200 ppm	−0.514	0.00185	−0.1325	0.0079	65.29
400 ppm	−0.525	0.00138	−0.1484	0.0057	74.11
600 ppm	−0.496	0.00106	−0.2153	0.0017	80.11
800 ppm	−0.494	0.00079	−0.2080	0.0009	85.18
1000 ppm	−0.500	0.00067	−0.2046	0.0003	87.43

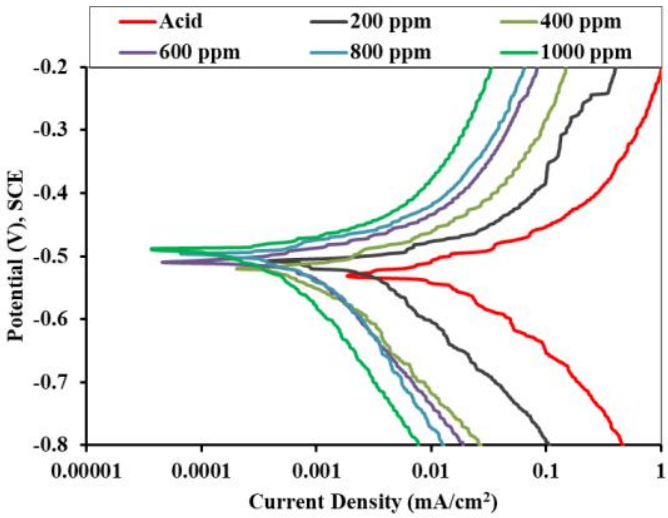

Figure 8. Potentiodynamic polarization curves for mild steel in 1 M H_2SO_4 containing different concentrations of inhibitor immersed condition.

In the corrosive media, the current density and the corresponding corrosion potential of MS were found to be 0.01246 mA/cm^2 and −0.526 V, respectively. A sudden drop in current density was induced by the addition of different concentrations of inhibitor solution. For the MS in the 1000 ppm inhibitor solution, the lowest current density observed was 0.00037 mA/cm^2, with the corresponding corrosion potential of −0.5 V. The inhibition efficiency, cathodic and anodic slope, corrosion potential, and corrosion current densities of the alkaloid for the 3 h immersed sample are tabulated in Table 4.

Table 4. Table showing the anodic slope, cathodic slope, and inhibition efficiency for the 3 h immersed sample.

Medium	OCP (V)	Anodic Slope (V/decade)	Cathodic Slope (V/decade)	I_{corr} (mA/cm^2)	I.E. (%)
Acid	−0.526	0.0761	−0.1416	0.01246	-
200 ppm	−0.515	0.0558	−0.1646	0.00268	78.49
400 ppm	−0.528	0.0621	−0.2023	0.00098	92.13
600 ppm	−0.505	0.0624	−0.2167	0.00086	93.10
800 ppm	−0.505	0.0617	−0.1958	0.00068	94.54
1000 ppm	−0.500	0.0551	−0.1944	0.00037	97.03

The polarization approach was used to assess the inhibition efficacy of various concentrations of inhibitor media for both immersed and as-immersed samples. The preceding tables (Tables 3 and 4) provide the experiment's efficiency matrices, from which it was observed that the inhibitor's inhibition efficacy was better for MS in as-immersed than that in 3 h immersion condition. Figure 9 depicts the variance in inhibitor effectiveness with varied concentrations for MS in both the immersed and as-immersed circumstances. The maximum efficiency was found to be 87.43% and 97.03% in the as-immersed and 3 h in the immersed MS samples, respectively, in a 1000 ppm inhibitor solution.

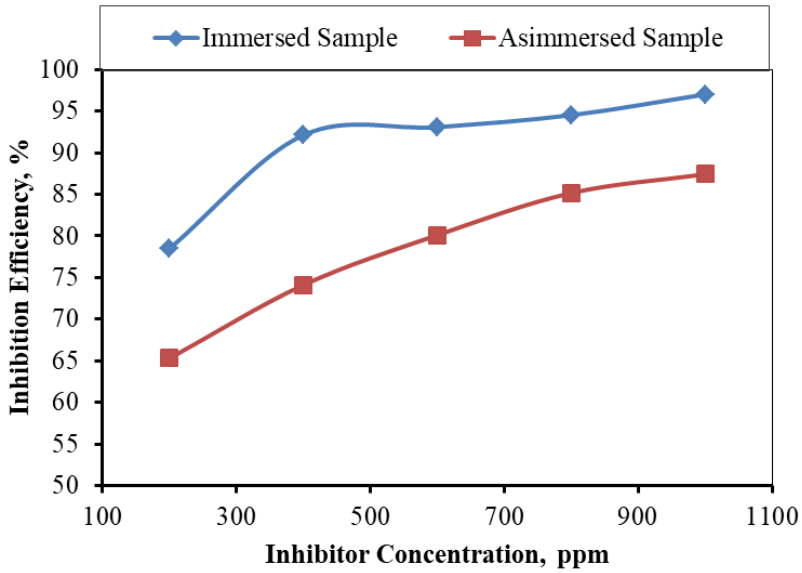

Figure 9. The inhibition efficiency of the inhibitor obtained from the polarization of both immersed and as-immersed MS samples in different concentrations of inhibitor.

4. Discussion and Mechanism of Corrosion Inhibition

Corrosion inhibition by CNSA molecules was studied by weight loss measurement method for which the effect of CNSA concentration and immersion time has been studied. A study on the effect of immersion time reveals that the CNSA inhibitor could work efficiently for any concentration up to 6 h immersion time. The efficiency of the lower concentrated inhibitor solutions subsequently decreases, which could be due to the formation of a chelate complex, as shown in Scheme 3 [6]. However, the inhibition efficiency of the inhibitor solutions of a higher concentration (800 and 1000 ppm) is almost similar and very high even for the 24 h immersed samples.

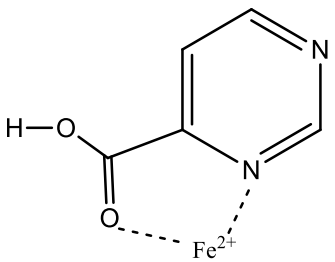

Scheme 3. Fe-Alkaloid Chelate Complex.

The study on the CNSA concentration indicated that 400 ppm and more concentration of an inhibitor is sufficient for corrosion inhibition. Corrosion inhibition is due to the adsorption of those molecules on the MS surface. The slope and R^2 values from the Langmuir adsorption isotherm showed that the monolayer of the CNSA adsorbed onto the MS surface. It is quite interesting that it is only possible for the adsorption of alkaloids

with molecular thickness. However, XPS or a sophisticated thickness measurement tool could be recommended for further verification.

Similarly, the free energy obtained reveals that adsorption is a chemical-dominated physical mechanism. It means the adsorption between the MS and CNSA could be due to the van der Waals forces and electrostatic attraction followed by the formation of a coordinate covalent bond with the metal d-orbital [25]. The negative value of the free energy indicates the spontaneous process of the adsorption of the inhibitor molecules. Simply, it reflects that no external energy is needed during the adsorption of the CNSA molecules on the MS surface. This helps to conclude that this CNSA could perform well in terms of commercialization.

Corrosion inhibition by alkaloid molecules is due to the adsorption of inhibitor molecules on the MS surface by replacing water molecules.

$$\mathrm{Org(sol) + xH_2O(ads) \rightleftharpoons Org(ads) + H_2O(sol)}$$

Org(sol) and Org(ads) represent the solvated and adsorbed alkaloid molecules, respectively. Similarly, H_2O(ads) represents the adsorbed water molecules on the MS surface, and x represents the number of water molecules replaced by one organic molecule [37].

At the very beginning, the heteroatom, particularly the nitrogen of the CNSA, becomes protonated in acid, due to which the acid molecules are less available for the deterioration of the MS surface. Due to the protonation, the sulfate ions roam freely in the solution and interact with the MS surface to form a thin sulfate layer. Then, the protonated alkaloid molecules simultaneously interact with the sulfate layer by the electrostatic force of attraction, thus producing a double-protective CNSA layer through the exchange mechanism. After that, a transformation of protonated alkaloids into neutral alkaloids takes place by H_2 gas evolution [25].

This is further supported by OCP and polarization results. OCP reflects the information regarding the positively or negatively charged MS surface. The OCP of the MS in acid-only solution is recorded around -0.526 V, which shifted more positively in the presence of indicators. This implies that the MS surface is positively charged [38]. On a positively charged surface, the interaction of SO_4^{2-} ions takes place through the electrostatic force of attraction, and the surface becomes negatively charged. Then, the protonated alkaloids could interact with the sulfate ions, which return to their neutral form after releasing H_2 molecules [37–39].

The cathodic slope of the polarization curves for both immersed and as immersed conditions are found to be parallel, i.e., no change in the slope trend. This indicates that the reaction mechanism was not changed with the addition of CNSA to the solutions, and the hydrogen evolution during the process is activation-controlled [40,41]. It was also found that the anodic and cathodic slopes of the polarization curves have not been changed upon the addition of CNSA. This indicates that the inhibition is due to the adsorption of CNSA molecules on the MS surface, entirely blocking the sites [42,43].

Here, the coordinate covalent bond between the nitrogen of the alkaloid molecule and the MS surface is formed due to the sharing of lone pair of an electron located at the HOMO with the vacant d-orbital of iron. The accumulated extra negative charge on the MS surface then returned to LUMO with high orbital density to attain stability. The steps of the corrosion inhibition mechanism [37] and the schematic diagram concerning the 4-pyrimidine carboxylic acid molecule are shown in Scheme 4.

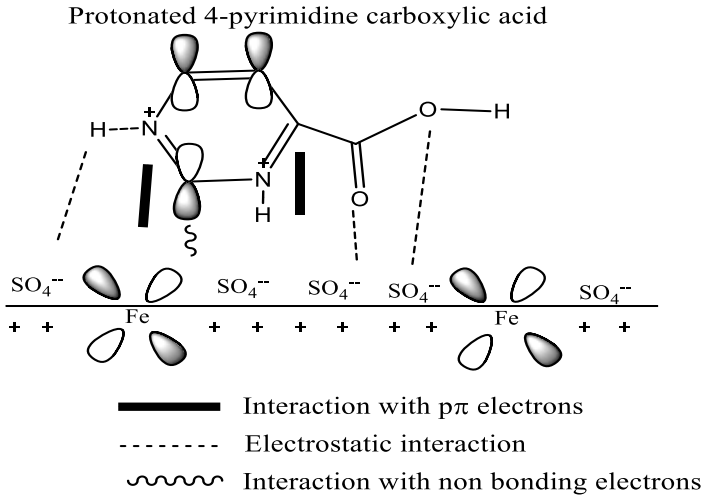

Scheme 4. Mechanism of corrosion inhibition by CNSA molecules in the reference of 4-pyrimidine carboxylic acid.

5. Conclusions

The extraction and characterization of CNSA were carried out successfully and efficiently. Gravimetric and electrochemical methods determined the corrosion inhibition efficacy of the extracted CNSA. The maximum inhibition efficiency of the CNSA by the gravimetric method was 96.41% and by electrochemical polarization was 97.03% achieved for the 1000 ppm inhibitor concentration. The data best fitted for the Langmuir adsorption isotherm, which reflects the monolayer formation tendency of the CNSA with intermediate free energy value. The extracted CNSA can be used as a good inhibitor to prevent corrosion in the industrial cleaning processes because of its promising efficiency.

Author Contributions: Conceptualization, H.B.O. and D.P.B.; methodology, H.B.O.; software, H.B.O.; validation, H.B.O. and D.P.B.; formal analysis, H.B.O.; investigation, N.K., A.S. and H.B.O.; resources, D.P.B.; data curation, D.P.B.; writing—original draft preparation, J.T.M. and H.B.O.; writing—review and editing, D.P.B. and B.P.; visualization, D.P.B.; supervision, D.P.B.; project administration, D.P.B.; funding acquisition, B.P. All authors have read and agreed to the published version of the manuscript.

Funding: This research received no external funding.

Institutional Review Board Statement: Not applicable.

Informed Consent Statement: Not applicable.

Data Availability Statement: Not applicable.

Conflicts of Interest: The authors declare no conflict of interest.

References

1. Davis, J.R. *Corrosion: Understanding the Basics*; Asm International: Almere, The Netherlands, 2000; ISBN 1-61503-068-9.
2. Yaro, A.S.; Khadom, A.A.; Wael, R.K. Apricot juice as green corrosion inhibitor of mild steel in phosphoric acid. *Alex. Eng. J.* **2013**, *52*, 129–135. [CrossRef]
3. El-Lateef, H.M.A.; Abo-Riya, M.A.; Tantawy, A.H. Empirical and quantum chemical studies on the corrosion inhibition performance of some novel synthesized cationic gemini surfactants on carbon steel pipelines in acid pickling processes. *Corros. Sci.* **2016**, *108*, 94–110. [CrossRef]
4. Oguzie, E. Corrosion inhibition of aluminium in acidic and alkaline media by *Sansevieria trifasciata* extract. *Corros. Sci.* **2007**, *49*, 1527–1539. [CrossRef]
5. Chapagain, A.; Acharya, D.; Das, A.K.; Chhetri, K.; Oli, H.B.; Yadav, A.P. Alkaloid of *Rhynchostylis retusa* as Green Inhibitor for Mild Steel Corrosion in 1 M H_2SO_4 Solution. *Electrochem* **2022**, *3*, 211–224. [CrossRef]
6. Dhakal, K.; Bohora, D.; Bista, B.; Oli, H.; Singh, S.; Bhattarai, D.; Karki, N.; Yadav, A. Alkaloids extract of Alnus nepalensis bark as a green inhibitor for mild steel corrosion in 1 M H_2SO_4 solution. *J. Nepal Chem. Soc.* **2022**, *43*, 76–92. [CrossRef]
7. Singh, W.P.; Bockris, J. Toxicity Issues of Organic Corrosion Inhibitors: Applications of QSAR Model. In *CORROSION 96*; OnePetro: Richardson, TX, USA, 1996.

8. Stupnišek-Lisac, E.; Bozic, A.L.; Cafuk, I. Low-Toxicity Copper Corrosion Inhibitors. *Corrosion* **1998**, *54*, 713–720. [CrossRef]
9. Rani, B.E.A.; Basu, B.B.J. Green Inhibitors for Corrosion Protection of Metals and Alloys: An Overview. *Int. J. Corros.* **2012**, *2012*, 380217. [CrossRef]
10. Asipita, S.A.; Ismail, M.; Majid, M.Z.A.; Majid, Z.A.; Abdullah, C.; Mirza, J. Green *Bambusa Arundinacea* leaves extract as a sustainable corrosion inhibitor in steel reinforced concrete. *J. Clean. Prod.* **2014**, *67*, 139–146. [CrossRef]
11. Qiang, Y.; Zhang, S.; Tan, B.; Chen, S. Evaluation of Ginkgo leaf extract as an eco-friendly corrosion inhibitor of X70 steel in HCl solution. *Corros. Sci.* **2018**, *133*, 6–16. [CrossRef]
12. Sexena, A.; Prasad, D.; Haldhar, R. Use of *Butea monosperma* Extracts as Green Corrosion Inhibitor for Mild Steel in 0.5 MH_2SO_4. *Int. J. of Electrochem. Sci.* **2017**, *12*, 8793–8805. [CrossRef]
13. Kamal, C.; Sethuraman, M. Caulerpin—A bis-Indole Alkaloid As a Green Inhibitor for the Corrosion of Mild Steel in 1 M HCl Solution from the Marine Alga *Caulerpa racemosa*. *Ind. Eng. Chem. Res.* **2012**, *51*, 10399–10407. [CrossRef]
14. Raja, P.B.; Fadaeinasab, M.; Qureshi, A.K.; Rahim, A.A.; Osman, H.; Litaudon, M.; Awang, K. Evaluation of Green Corrosion Inhibition by Alkaloid Extracts of *Ochrosia oppositifolia* and Isoreserpiline against Mild Steel in 1 M HCl Medium. *Ind. Eng. Chem. Res.* **2013**, *52*, 10582–10593. [CrossRef]
15. Raja, P.B.; Qureshi, A.K.; Rahim, A.A.; Osman, H.; Awang, K. *Neolamarckia cadamba* alkaloids as eco-friendly corrosion inhibitors for mild steel in 1M HCl media. *Corros. Sci.* **2013**, *69*, 292–301. [CrossRef]
16. Ikeuba, A.; Okafor, P.; Ekpe, U.; Ebenso, E.E. Alkaloid and Non-Alkaloid Ethanolic Extracts from Seeds of *Garcinia kola* as Green Corrosion Inhibitors of Mild Steel in H_2SO_4 Solution. *Int. J. Electrochem. Sci.* **2013**, *8*, 7455–7467.
17. Ugi, B.U. Alkaloid and Non Alkaloid Extracts of Solanum melongena Leaves as Green Corrosion Inhibitors on Carbon Steel in Alkaline Medium. *Fountain J. Nat. Appl. Sci.* **2014**, *3*. [CrossRef]
18. Faustin, M.; Maciuk, A.; Salvin, P.; Roos, C.; Lebrini, M. Corrosion inhibition of C38 steel by alkaloids extract of Geissospermum laeve in 1M hydrochloric acid: Electrochemical and phytochemical studies. *Corros. Sci.* **2015**, *92*, 287–300. [CrossRef]
19. Ngouné, B.; Pengou, M.; Nouteza, A.M.; Nanseu-Njiki, C.P.; Ngameni, E. Performances of Alkaloid Extract from *Rauvolfia macrophylla* Stapf toward Corrosion Inhibition of C38 Steel in Acidic Media. *ACS Omega* **2019**, *4*, 9081–9091. [CrossRef]
20. Sadik, K.; Hamdani, N.E.; Hachim, M.; Byadi, S.; Bahadur, I.; Aboulmouhajir, A. Towards a Theoretical Understanding of Alkaloid-Extract Cytisine Derivatives of *Retama monosperma* (L.) Boiss. Seeds, as Eco-Friendly Inhibitor for Carbon Steel Corrosion in Acidic 1M HCl Solution. *J. Theor. Comput. Chem.* **2020**, *19*, 2050013. [CrossRef]
21. Parajuli, D.; Sharma, S.; Oli, H.B.; Bohara, D.S.; Bhattarai, D.P.; Tiwari, A.P.; Yadav, A.P. Comparative Study of Corrosion Inhibition Efficacy of Alkaloid Extract of *Artemesia vulgaris* and *Solanum tuberosum* in Mild Steel Samples in 1 M Sulphuric Acid. *Electrochem* **2022**, *3*, 416–433. [CrossRef]
22. Lebrini, M.; Robert, F.; Roos, C. Inhibition Effect of Alkaloids Extract from *Annona Squamosa* Plant on the Corrosion of C38 Steel in Normal Hydrochloric Acid Medium. *Int. J. Electrochem. Sci.* **2010**, *5*, 1698–1712.
23. Lebrini, M.; Robert, F.; Roos, C. Alkaloids Extract from *Palicourea guianensis* Plant as Corrosion Inhibitor for C38 Steel in 1 M Hydrochloric Acid Medium. *Int. J. Electrochem. Sci.* **2011**, *6*, 847–859.
24. Lecante, A.; Robert, F.; Blandinières, P.; Roos, C. Anti-corrosive properties of *S. tinctoria* and *G. ouregou* alkaloid extracts on low carbon steel. *Curr. Appl. Phys.* **2011**, *11*, 714–724. [CrossRef]
25. Karki, R.; Bajgai, A.K.; Khadka, N.; Thapa, O.; Mukhiya, T.; Oli, H.B.; Bhattarai, D.P. *Acacia catechu* Bark Alkaloids as Novel Green Inhibitors for Mild Steel Corrosion in a One Molar Sulphuric Acid Solution. *Electrochem* **2022**, *3*, 668–687. [CrossRef]
26. Hanini, K.; Benahmed, M.; Boudiba, S.; Selatnia, I.; Akkal, S.; Laouer, H. Experimental and Theoretical Studies of Taxus Baccata Alkaloid Extract as Eco-Friendly Anticorrosion for Carbon Steel in Acidic Solution. *Prot. Met. Phys. Chem. Surfaces* **2021**, *57*, 222–233. [CrossRef]
27. Raja, P.B.; Qureshi, A.K.; Rahim, A.A.; Awang, K.; Mukhtar, M.R.; Osman, H. Indole Alkaloids of Alstonia angustifolia var. latifolia as Green Inhibitor for Mild Steel Corrosion in 1 M HCl Media. *J. Mater. Eng. Perform.* **2013**, *22*, 1072–1078. [CrossRef]
28. Guo, L.; Qiang, T.; Ma, Y.; Wang, K.; Du, K. Optimisation of tannin extraction from *Coriaria nepalensis* bark as a renewable resource for use in tanning. *Ind. Crop. Prod.* **2020**, *149*, 112360. [CrossRef]
29. Kumar, P.; Bhatt, R.; Singh, L.; Sati, O.; Khan, A.; Ahmad, A. Antimicrobial activities of essential oil and methanol extract of *Coriaria nepalensis*. *Nat. Prod. Res.* **2011**, *25*, 1074–1081. [CrossRef]
30. Zhao, F.; Liu, Y.; Ma, S.; Yu, D.; Yu, S. New compounds from the roots of *Coriaria nepalensis*. *Chin. Chem. Lett.* **2018**, *29*, 467–470. [CrossRef]
31. Wei, H.; Zeng, F.; Lu, M.; Tang, R. Studies on chemical constituents from the root of *Coriaria nepalensis* wall (*Coriaria sinica Maxim*). *Yao Xue Xue Bao Acta Pharm. Sin.* **1998**, *33*, 688–692.
32. Silverstein, R.M.; Bassler, G.C. Spectrometric identification of organic compounds. *J. Chem. Educ.* **1962**, *39*, 546. [CrossRef]
33. Sharma, Y.R. *Elementary Organic Spectroscopy*; S. Chand Publishing: New Delhi, India, 2007; ISBN 81-219-2884-2.
34. Andoor, P.A.; Okeoma, K.B.; Mbamara, U.S. Adsorption and Thermodynamic Studies of the Corrosion Inhibition Effect of Rosmarinus *Officinalis* L. Leaves on Aluminium Alloy in 0.25 M HCl and Effect of an External Magnetic Field. *Int. J. Phys. Sci.* **2021**, *16*, 79–95.
35. Karki, N.; Choudhary, Y.; Yadav, A.P. Thermodynamic, Adsorption and Corrosion Inhibition Studies of Mild Steel by Artemisia vulgaris Extract from Methanol as Green Corrosion Inhibitor in Acid Medium. *J. Nepal Chem. Soc.* **2018**, *39*, 76–85. [CrossRef]

36. Oli, H.B.; Parajuli, D.L.; Sharma, S.; Chapagain, A.; Yadav, A.P. Adsorption Isotherm and Activation Energy of Inhibition of Alkaloids on Mild Steel Surface in Acidic Medium. *Amrit Res. J.* **2021**, *2*, 59–67. [CrossRef]
37. Karki, N.; Neupane, S.; Gupta, D.K.; Das, A.K.; Singh, S.; Koju, G.M.; Chaudhary, Y.; Yadav, A.P. Berberine isolated from *Mahonia nepalensis* as an eco-friendly and thermally stable corrosion inhibitor for mild steel in acid medium. *Arab. J. Chem.* **2021**, *14*, 103423. [CrossRef]
38. Karki, N.; Neupane, S.; Chaudhary, Y.; Gupta, D.; Yadav, A. Equisetum Hyemale: A New Candidate for Green Corrosion Inhibitor Family. *Int. J. Corros. Scale Inhib.* **2021**, *10*, 206–227.
39. Karthik, R.; Muthukrishnan, P.; Chen, S.-M.; Jeyaprabha, B.; Prakash, P. Anti-Corrosion Inhibition of Mild Steel in 1M Hydrochloric Acid Solution by Using *Tiliacora accuminata* Leaves Extract. *Int. J. Electrochem. Sci.* **2015**, *10*, 3707–3725.
40. Chkirate, K.; Azgaou, K.; Elmsellem, H.; El Ibrahimi, B.; Sebbar, N.K.; Anouar, E.H.; Benmessaoud, M.; El Hajjaji, S.; Essassi, E.M. Corrosion inhibition potential of 2-[(5-methylpyrazol-3-yl)methyl]benzimidazole against carbon steel corrosion in 1 M HCl solution: Combining experimental and theoretical studies. *J. Mol. Liq.* **2021**, *321*, 114750. [CrossRef]
41. Tan, B.; Zhang, S.; He, J.; Li, W.; Qiang, Y.; Wang, Q.; Xu, C.; Chen, S. Insight into anti-corrosion mechanism of tetrazole derivatives for X80 steel in 0.5 M H_2SO_4 medium: Combined experimental and theoretical researches. *J. Mol. Liq.* **2021**, *321*, 114464. [CrossRef]
42. Fekkar, G.; Yousfi, F.; Elmsellem, H.; Aiboudi, M.; Ramdani, M.; Abdel-Rahman, I.; Hammouti, B.; Bouyazza, L. Eco-Friendly Chamaerops Humilis L. Fruit Extract Corrosion Inhibitor for Mild Steel in 1 M HCl. *Int. J. Corros. Scale Inhib.* **2020**, *9*, 446–459.
43. Hafez, B.; Mokhtari, M.; Elmsellem, H.; Steli, H. Environmentally Friendly Inhibitor of the Corrosion of Mild Steel: Commercial Oil of Eucalyptus. *Int. J. Corros. Scale Inhib.* **2019**, *8*, 573–585.